

KnowEEG: Explainable Knowledge Driven EEG Classification

Amarpal Sahota^{a,*}, Navid Mohammadi Foumani^b, Raul Santos-Rodriguez^a, Zahraa S. Abdallah^a

^a*University of Bristol, Bristol, United Kingdom*

^b*Monash University, Melbourne, Victoria, Australia*

Abstract

Electroencephalography (EEG) is a method of recording brain activity that shows significant promise in applications ranging from disease classification to emotion detection and brain-computer interfaces. Recent advances in deep learning have improved EEG classification performance yet model explainability remains limited. To address this key limitation we introduce KnowEEG; a novel explainable machine learning approach for EEG classification. KnowEEG extracts a comprehensive set of per-electrode features, filters them using statistical tests, and integrates between-electrode connectivity statistics. These features are then input to our modified Random Forest model (Fusion Forest) that balances per electrode statistics with between electrode connectivity features in growing the trees of the forest. By incorporating knowledge from both the generalized time-series and EEG-specific domains, KnowEEG achieves performance comparable to or exceeding state-of-the-art deep learning models across five different classification tasks: emotion detection, mental workload classification, eyes open/closed detection, abnormal EEG classification, and event detection. In addition to high performance, KnowEEG provides inherent explainability through feature importance scores for understandable features. We demonstrate by example on the eyes closed/open classification task that this explainability can be used to discover knowledge about the classes. This discovered knowledge

*Corresponding author.

Email addresses: amarpal.sahota@bristol.ac.uk (Amarpal Sahota), Navid.Foumani@monash.edu (Navid Mohammadi Foumani), enrsr@bristol.ac.uk (Raul Santos-Rodriguez), zahraa.abdallah@bristol.ac.uk (Zahraa S. Abdallah)

for eyes open/closed classification was proven to be correct by current neuroscience literature. Therefore, the impact of KnowEEG will be significant for domains where EEG explainability is critical such as healthcare.

1. Introduction

Electroencephalogram (EEG) is a widely used method of recording cortical neuronal activity with a high temporal resolution [1]. Data collection is relatively inexpensive and also non-invasive. Thus, EEG has great potential to drive advancements in mental health, enable sophisticated brain-computer interfaces, and enhance disease detection, paving the way for future innovations in healthcare. Extensive research has explored EEG classification with applications ranging from the classification of neurodegenerative diseases such as Alzheimer's [2] to motor task recognition for Brain-Computer Interfaces [3] and emotion detection [4].

EEG classification is a challenging task given the low signal-to-noise ratio in EEG signals and the presence of inter-subject variability requiring models to generalize well across individuals. Traditional machine learning methods for EEG classification have relied on standard hand-crafted features as inputs to models such as support vector machines, random forests or neural networks [5] [6]. These pipelines often use frequency-based features combined with select statistics of the EEG signal [2]. One key limitation for traditional feature-based methods has been poor performance in settings where prior knowledge is limited. For this reason, in the last decade research has focussed increasingly on deep learning methodologies.

Deep learning methods in this context range from convolutional neural networks (CNN) applied to the raw EEG data to audio-inspired networks that apply a CNN to EEG spectrograms (time-frequency image of the EEG) [7]. Recent advances in deep learning architectures have also led to transformer-inspired networks such as EEG Conformer [8] and EEG2Rep [9] (self-supervised representation-based model) for classification. Although the performance across EEG classification tasks has improved, deep learning models are often opaque and their inner workings are hard to interpret. This leads researchers to post-hoc explainability methods in an attempt to understand models [10]. Explainability is a particularly critical issue for EEG as it can enhance insights into neurophysiological phenomena, aid clinical decision-making and improve trust in the model.

Therefore, while data and compute hungry deep learning methods also have issues around explainability, existing feature-based methods struggle to achieve high classification performance across diverse EEG classification tasks. We revisit the overlooked domain of feature-based methods and present a novel feature based EEG classification pipeline KnowEEG that addresses these limitations achieving both high performance and explainability. We hypothesize that the informative feature space for EEG Classification tasks consists of per-electrode features combined with between-electrode connectivity measures. Thus, we construct KnowEEG to reflect this. We leverage existing time series and EEG knowledge to construct a large feature space of 783 per electrode statistics that are filtered and then combined with between electrode connectivity statistics. These features are input to our modified Random Forest model (Fusion Forest) that balances per electrode statistics with between electrode connectivity features in growing the trees of the forest (see pipeline in Figure 1 and Fusion Forest Algorithm 1). Utilizing a high dimensional feature space enables KnowEEG to achieve high performance across a diverse set of EEG classification tasks. Combining this performance with the explainability of our approach means KnowEEG can also be used to discover new knowledge about the classification task at hand.

In this paper, we present the full architecture of KnowEEG in Section 3. In Section 4.4, we present the results of KnowEEG versus state-of-the-art competitors across five different EEG classification task domains (Emotion detection, mental workload classification, eyes open/closed detection, Abnormal EEG classification, Event Detection), showing KnowEEG to exceed or match state of the art performance across tasks. Finally, in Section 4.5, we demonstrate the explainability benefits of KnowEEG and show that KnowEEG can be used to learn correct knowledge about the classification task being studied.

2. Related Work

In this section, we present related work which includes feature-based methods for general time series classification (across domains), feature based methods for EEG classification, and deep learning for EEG classification.

2.1. Feature Engineering for General Time Series

Time series data covers vastly different domains from energy consumption to EEG and weather prediction. Although different, all domains share the

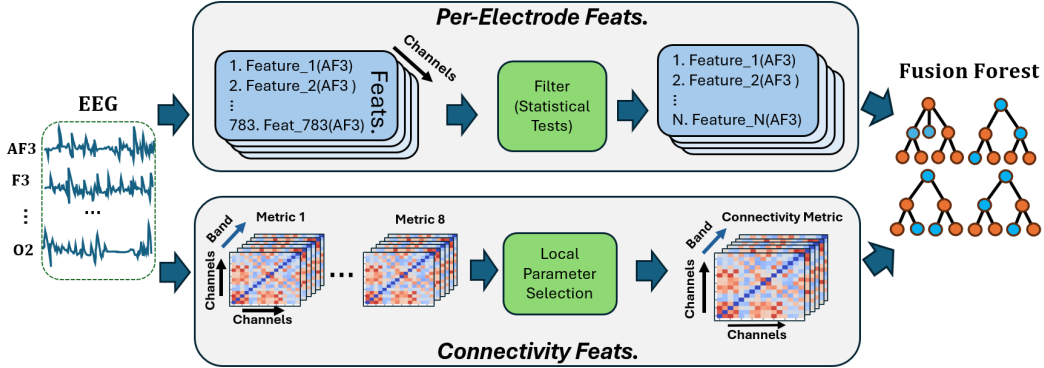


Figure 1: KnowEEG Pipeline: There are two parallel threads to the pipeline. In thread one, 783 features from generalised and EEG-specific time-series literature are calculated per electrode and concatenated. Feature relevance is evaluated via univariate non-parametric hypothesis tests (Mann-Whitney U for binary targets and Kruskal-Wallis tests for multiclass targets), with Benjamini–Yekutieli correction to control the false discovery rate ($\alpha = 0.05$), filtering out uninformative features. In thread two, between-electrode connectivity features are calculated for connectivity metrics. The best-performing metric is selected using classifier performance on the validation data. The features from thread one and thread two are then combined using the Fusion Forest (see Algorithm 1).

fundamental property of sequentially ordered observations that change over time. Basic statistical descriptors such as mean, variance, skewness and kurtosis are often used as a starting point for classification. Features can then be extended to temporal patterns which include autocorrelation at different lags, peak detection and peak counting among others. In [11], the authors propose a set of 22 features for generalized time series classification after extensive testing on 93 time series datasets. The ‘catch22’ features include linear and non-linear autocorrelation, successive differences, value distributions and outliers and fluctuation scaling properties [11]. Features for generalized time series classification can also include shape-based features such as shapelets or motifs that capture local patterns. Finally, features can also be generated from the frequency domain. These are discussed in detail in 2.2.

2.2. Feature Engineering for EEG

Research has shown frequency-based features to be particularly informative of brain activity [12] and therefore effective for EEG classification. The power spectral density (strength of the EEG signal across frequencies) is calculated using the Fourier transform. From the power spectral density band powers and peak frequency values can be calculated. Band powers refer to

specifically defined frequency bands. For our paper we use the band power definitions as delta (0.5–4Hz), theta (4–8Hz), alpha (8–12Hz), sigma (12–16Hz), beta (16–30Hz) and gamma (30–40Hz). Band power values and peak / median frequency features can be input to machine learning models such as support vector machines or random forests for classification as in [5] and [6].

The afore-discussed features though effective reduce temporal resolution to the window over which the feature was calculated and discard phase information within the signal. Connectivity measures are metrics for calculating connectivity between regions of the brain and often utilize phase information. Phase Lag Index (PLI) for example [13], measures the asymmetry of the distribution of phase differences across time between two signals with its value ranging between 0 and 1. A PLI of zero means no coupling (or instantaneous coupling) and a value of 1 means true lagged interaction. Connectivity measures can be calculated for the entire EEG signal between electrodes or for sub-components of the EEG signal within the frequency domain (commonly band powers). For example in [13], researchers find the phase lag index in the alpha band to be correlated with cognitive assessment score in the task of Mild Cognitive Impairment classification.

Brain connectivity in general comprises the following subcomponents; structural connectivity (anatomical connectivity between brain regions), functional connectivity (statistical dependencies or correlations in activity) and effective connectivity (causal or directional influences between regions) [14]. Another commonly used metric is coherence which measures functional connectivity via correlation in the frequency domain. In [15] researchers use coherence combined with other signal statistics to achieve over 90% accuracy in the task of Parkinson’s classification.

Thus, in summary, feature-based approaches inspired by domain knowledge have been successful for EEG classification often focusing on frequency-based properties of the signal and measures of connectivity across the brain. While many feature-engineering approaches exist, none provide a unified, high-performance, explainable pipeline applicable across multiple EEG classification domains.

2.3. Deep Learning for EEG

Over the last decade, deep learning has experienced unprecedented growth and success across domains. This has led to much research experimenting

with existing deep learning architectures applied to EEG data and the development of EEG-specific deep neural architectures[9].

Firstly, researchers have effectively applied simple convolutional neural networks (CNNs) directly to processed EEG data for classification. In [7] a CNN comprising of a series of 1D-convolutions and max pooling layers achieved just under 90% accuracy on Parkinson’s classification. EEG researchers have since taken inspiration from the audio domain by applying CNNs to time-frequency images (spectrograms) of the raw EEG signal [16] [17].

Deep learning architectures have also been developed to deal directly with sequential data from RNN variants such as LSTMs and GRU’s to more recently Transformers. Transformers excel at capturing long-range dependencies and as such have been successfully used for EEG classification. In [18] the authors present a novel architecture that uses a convolutional module to generate embeddings for input EEG data which is then passed to a Transformer Encoder module for classification. This EEG Conformer achieves state of the art performance on many brain computer interface based tasks [18].

One issue with deep neural networks is susceptibility to over-fitting [9]. With EEG data this is particularly problematic as signals are noisy and inter-subject variability can be present [19]. Self-supervised learning (SSL) aims to solve this problem by learning a representation of the EEG and generating a self-supervisory signal from the data [20]. These models can learn from labelled or unlabeled data and the learnt representations used for classification. State-of-the-art SSL deep learning models include BENDR [21], BIOT [22] and most recently EEG2Rep [9].

Thus, in summary, many deep learning models have been applied to and developed specifically for EEG data. Deep learning has been successful in the classification of EEG. However, explainability remains an issue with deep learning models being opaque and there is yet to be a model that is effective across task domains.

3. Methodology of KnowEEG

3.1. Problem Statement

We address the problem of EEG classification. Each EEG sample X_i from a dataset $\{X_1, X_2, \dots, X_N\}$ maps to a corresponding label y_i from the set $\{y_1, y_2, \dots, y_N\}$. The label is a scalar value corresponding to the class of each

respective sample. Each EEG sample X_i is multi-dimensional consisting of K electrode channels each with a sequence length of L .

Our goal is to learn an explainable high-performance classifier that can map samples X_i to labels y_i . This is primarily measured with performance. Accuracy and AUROC are used as performance metrics for binary classification. Balanced Accuracy and Weighted F1 Score are used for multi-class classification. Explainability is established via generating understandable features and using a tree-based model that provides direct access to feature importances. The explainability of KnowEEG is demonstrated in 4.5.

3.2. KnowEEG Model Architecture

Thread One : per electrode features.

Per electrode we calculate 783 features from both the generalized time series domain and the EEG-specific domain. This includes basic features like mean, standard deviation and kurtosis to more complex time series features like autocorrelation at different lags and EEG specific features related to frequency components present in the signal. In order to do this calculation the time series Python package TSFresh [23] is used. Exact settings for feature calculation are presented in 4.3 and further details for implementation provided in Appendix A. These per electrode features are concatenated after being calculated. Therefore, for our 14 electrode datasets there are 783 features x 14 electrodes which equals 10,962 time series features per sample (12,528 for 16 electrode datasets). Our aim is to create a broad set of time series descriptors for each EEG sample. We hypothesize that this broad set of features contains the subset of informative features for the specific EEG classification task. To avoid model over-fitting and reduce unnecessary computation, features are filtered using univariate non-parametric hypothesis tests to assess their relevance to the classification target. For binary classification we use the Mann-Whitney U test while for multi-class classification Kruskal-Wallis tests are applied. Resulting p-values are adjusted to control the false discovery rate using the Benjamini-ekutieli correction, with a significance threshold of 0.05 [24]. Thus, the per electrode thread of the pipeline results in a final set of filtered per electrode features as shown in Figure 1.

Thread Two: between electrode connectivity features.

We calculate a separate set of between electrode connectivity features. We select Spearman and Pearson correlation, which measure linear and non-

linear correlation between electrodes. For a 14 electrode dataset this results in 182 correlation features (91 Spearman and 91 Pearson). We also select a series of well researched EEG specific connectivity measures. For our pipeline we select Coherence (Coh) , Imaginary Coherence (ImCoh), Pairwise Phase Consistency (PPC), Phase Lag Value (PLV), Phase Lag Index (PLI) , Directed Phase Lag Index (DPLI) and Weighted Phase Lag Index (WPLI) [25]. Users of the pipeline can select any number of connectivity metrics that they expect could be informative for classification. These connectivity metrics can be calculated for the entire signal or on sub components of the signal. We propose calculating these metrics for each sub band of the EEG signal with regards to the bands defined in 2.2. Therefore per connectivity metric, for the 14 electrode datasets there are 91 (features per sub band) x 6 sub bands (delta, theta, alpha, sigma, beta, gamma) which equates to 546 total features per metric (720 features for 16 electrode datasets). These connectivity metrics require segmentation of the raw signal into epochs prior to calculation. We follow standard protocol for segmentation and detail this in Appendix C. In addition to these conventional connectivity metrics we also define Functional Power Connectivity (FPC) which consists of per electrode relative band powers and electrode-electrode features capturing spatial differences in oscillatory power across brain regions. Unlike phase-based metrics, FPC can be computed reliably even from short signals where windowing introduces noise. See Appendix B for full FPC definition. Therefore, in total we have 9 candidate connectivity metrics.

We consider selection of a single connectivity metric in this thread of the pipeline as a hyperparameter. We propose selecting a single connectivity metric as opposed to selecting some features from all metrics for ease of interpretability. This hyperparameter is selected using 'local parameter selection' in order to reduce the computational requirement of KnowEEG. Local parameter selection means that only the connectivity data is being used for parameter selection and not the per electrode statistics. A default 100 tree Random Forest model is used to select the highest performing connectivity metric on the validation set, fitting to each connectivity metric one at a time and testing performance on the validation set as shown in Figure 1 .

Feature Fusion: per-electrode and between electrode features.

We now have per electrode features from thread one and between electrode features (connectivity measure) from thread two of the pipeline. We consider this data to be of two different 'modes' and thus require a method

Algorithm 1 The Fusion Forest Algorithm. This modified Random Forest balances two feature modes (X_a and X_b) by independently selecting a random subset of features from each (lines 5-6) before fitting each of the K trees. This prevents the feature set with a higher dimension from dominating the model.

- 1: **Input:** N samples, X_a with A total features (mode 1), X_b with B total features (mode 2)
- 2: Select number of trees K for the Fusion Forest
- 3: **for** $k = 1$ to K **do**
- 4: Select random subset of samples N_{subset} (bootstrap sample of size N)
- 5: Select a random subset of \sqrt{A} features from X_a giving $X_{a\text{subset}}$
- 6: Select a random subset of \sqrt{B} features from X_b giving $X_{b\text{subset}}$
- 7: Fit a Decision Tree to $(N_{\text{subset}}, X_{a\text{subset}}, X_{b\text{subset}})$
- 8: Add the Decision Tree to the Fusion Forest
- 9: **end for**

of combining the information from both modes. For a classifier we select the Random Forest as it is inherently explainable and has been shown to perform well on EEG classification from features [26] [27]. For fusion of the two modes we can select feature level fusion, decision level fusion or propose another method. As the number of features per electrode can be far higher than the number of connectivity metrics we decide against feature level fusion as for tree-based models (especially Random Forests) this can skew the model towards the mode with more features. Decision-level fusion would be viable. However, we hypothesize that highest performance will be achieved if each tree in the Random Forest has access to features from both modes of data. We thus propose a modification of the traditional Random Forest algorithm so that for each tree a random subset of features is selected from mode 1 and separately from mode 2. We have not seen this simple modification to the Random Forest for feature fusion in the literature and therefore we outline the algorithm for this in 1. We call this the Fusion Forest.

4. Experiments and Discussion

4.1. Datasets

We use five publicly available EEG datasets. Three of the datasets recorded data with 14 channel Emotiv EEG headsets. These datasets are

DREAMER (emotion detection) [4] , STEW (Mental workload Classification) [28] and Crowdsourced (eyes open / close detection) [29]. EEG from these datasets had a sampling rate of 128Hz upon recording and all samples are two seconds long (after pre-processing). Recorded data for these three datasets is processed as per [9], snipping the data to create 2 second segments. Further details are provided in Appendix D.

The other two datasets are from the Temple University Hospital (TUH) Corpus [30] [31]. TUH is one of the largest EEG data repositories in the world with data collected in a lab setting with a range of different EEG recording devices. In processing this data we select 16 standard EEG channels following the 10-20 international system. This data was recorded at 256Hz with 5 second samples for TUEV [31] and 10 second samples for TUAB [30]. We provide further details of processing in Appendix Appendix D.

The Emotiv datasets were split into train / validation / test sets subject wise, challenging models to learn generalizable patterns across subjects. The TUH datasets (TUEV and TUAB) were inherently split already into train and test sets. We further split the train sets into 80% training and 20% validation. Again, this is following the same protocol as in [9].

Table 1 shows the main characteristics of all five data sets. Further information on each dataset and pre-processing can be found in Appendix D.

Table 1: Properties of the EEG datasets used (adapted from [9]). DREAMER [4], STEW [28], Crowdsourced [29], TUEV [31] and TUAB [30]

Dataset	Classification Task	Dim.	Freq.	Duration	Samples
DREAMER	Emotion Detection	14	128Hz	2s	77,910
STEW	Mental Workload	14	128Hz	2s	26,136
Crowdsourced	Eyes Open/Closed	14	128Hz	2s	12,296
TUEV	Event Detection	16	256Hz	5s	112,464
TUAB	Abnormal EEG	16	256Hz	10s	409,455

4.2. State-of-the-art Methods

We compare our pipeline to many state-of-the-art methods from the literature. Recent research has seen representation based deep learning methods

excel on EEG data [21][9]. Thus we compare versus four deep learning representation based classification models. The recently developed EEG2Rep [9] as well as BIOT [22], BENDR [21] and MAEEG [32]. Per [9] these self-supervised models achieve the highest performance if they are first able to learn a representation of the EEG by training on the data in a self-supervised fashion without labels before being trained on the data with labels. This is referred to as the ‘Fine Tuning’ setting. Thus, we deploy these models in this fine-tuning fashion where they perform best. We deploy EEG2Rep in both the fine-tuning fashion and the default fashion where it is deployed directly on the data without a pre-training phase. We also select the EEG Conformer [8] as a competitor model (deep learning model for classification). This model is adapted from transformer architecture. Finally, we select a general time series feature-based method, Catch22 [11]. These models were all implemented using publicly available code to ensure fair evaluation.

4.3. Experimental Procedure

For all datasets our pipeline KnowEEG (see 3) and all competitor models (see 4.2) were trained on the training split of the dataset, had hyperparameters tuned using the validation dataset and were tested on a holdout test set. This was done for five different random seeds. Mean and standard deviation of performance metrics were used to assess model performance. For binary classification, accuracy and Area Under ROC Curve (AUROC) are selected as the performance metrics. For multi-class classification on the TUEV dataset Balanced Accuracy and Weighted F1 score are used. This is the exact same experimental procedure as in [9].

For KnowEEG the TSFresh [23] package is used with ‘Efficient’ settings to calculate per electrode statistics. The MNE Python package [25] is used for calculating connectivity metrics. For the Fusion Forest the number of trees hyperparameter was selected from the list [50,100,200,500, 800, 1000]. Further details for the set up of KnowEEG are provided in Appendix A.

4.4. Results

Table 2 shows the average performance for all models across the DREAMER, Crowdsourced, STEW, TUEV and TUAB datasets. With 10 total performance metrics across 5 datasets KnowEEG achieves best performance vs. all other models on 5/10 metrics, second best on 4/10 (with 2/10 not significantly worse than the best model) and third best on 1/10 metrics. Thus,

judging by performance ranking alone, KnowEEG is the best performing model overall versus state-of-the-art competitors.

Crowdsourced is the EEG task where models perform best with the task of classifying eyes open vs eyes closed EEG data. On this dataset, KnowEEG has the second highest accuracy with 92.81 % performing marginally worse than the pre-trained EEG2Rep model. For AUROC KnowEEG outperforms all other models with 96.72 and performs consistently across seeds with a small standard deviation of only 0.21. Notably, the other feature based method Catch22 [11] performs well on this dataset achieving 89.57 % accuracy and 95.82 AUROC (second best). However, Catch22 performs poorly on all other datasets illustrating that traditional feature-based methods can struggle to perform well across a diverse set of EEG classification tasks.

On STEW with the task of mental workload classification KnowEEG significantly outperforms all other models in both accuracy and AUROC with standard deviations of under 1 for both metrics again illustrating consistent performance across seeds. On DREAMER performance is more variable across seeds and closer to other models. However, KnowEEG still performs best in accuracy (though not significantly) and second best in AUROC (again not significant).

For the TUEV dataset KnowEEG is third in balanced accuracy yet significantly outperforms all other models in weighted F1 score. TUEV is an extremely unbalanced dataset with 6 classes of EEG events. Therefore in this case balanced accuracy is not necessarily the best measure of overall model performance. This is because balanced accuracy ignores class distributions resulting in smaller classes having a disproportional impact on the balanced accuracy score and can be a drawback if targeting good accuracy on the entire dataset[33]. Weighted F1-score combines both precision and recall with each class weighted proportionally. Thus, it is notable that KnowEEG outperforms all other models in this metric significantly.

For abnormal EEG classification on TUAB KnowEEG performs second best to EEG2Rep on both accuracy and AUROC. However KnowEEG is within the standard deviation of EEG2Rep so this result is not significant. BIOT also reaches the same performances as EEG2Rep and KnowEEG when accounting for standard deviation across runs.

EEG2Rep Pre-trained [9] is overall the second best performing model achieving best performance or second best performance on 8/10 metrics across the five datasets. Besides performance, when compared with Deep Learning models, KnowEEG has the significant advantage of not requiring

GPU for training. All self-supervised representation-based models (except EEG2Rep Default) were trained first on the training data in self-supervised fashion and then tuned in supervised fashion. This requires significant GPU resource, in particular for the larger datasets. KnowEEG does not require any GPU resource. KnowEEG also has the significant advantage of using calculated features that are inherently interpretable and a tree-based model which enables users to access feature importances directly. We demonstrate the benefits of this explainability in Section 4.5.

Table 2: Performance of KnowEEG versus competitor models across datasets. KnowEEG results are shaded in blue. Best performance per dataset is in **bold** with second best underlined with Accuracy results in table a) and AUROC in table b).

(a) Accuracy (Acc) Performance

Models	DREAMER Acc	Crowdsourced Acc	STEW Acc	TUEV B-Acc	TUAB Acc
BENDR	54.45±2.11	83.78±2.35	69.74±2.11	41.17±2.89	76.96±3.98
MAEEG	53.63±2.61	86.75±3.50	72.46±3.67	41.23±3.65	77.56±3.56
BIOT	53.45±2.01	87.95±3.52	69.88±2.15	<u>46.02</u> ±1.68	79.21±2.15
Catch22	59.06±1.61	89.57±0.64	55.72±0.2	33.65±0.5	69.84±1.06
EEGConformer	55.40±2.76	87.62±2.91	<u>74.35</u> ±1.88	43.88±1.62	78.36±1.71
EEG2Rep (Default)	54.61±2.22	91.19±1.18	70.26±1.59	44.25±3.01	77.85±3.14
EEG2Rep (Pre-Trained)	<u>60.37</u> ±1.52	94.13 ±1.21	73.60±1.47	52.95 ±1.58	80.52 ±2.22
KnowEEG	61.53 ±2.59	<u>92.81</u> ±0.32	77.86 ±0.19	45.06±0.71	<u>80.18</u> ±0.24

(b) AUROC Performance

Models	DREAMER AUROC	Crowdsourced AUROC	STEW AUROC	TUEV W-F1	TUAB AUROC
BENDR	53.02±1.31	83.80±2.63	69.77±2.03	67.31±2.96	83.97±3.44
MAEEG	52.08±2.36	86.21±3.41	72.50±3.22	67.38±3.69	86.56±3.33
BIOT	53.53±1.82	87.78±3.09	70.11±2.57	69.98±1.99	87.42±2.01
Catch22	51.6±2.17	<u>95.82</u> ±0.3	53.2±0.14	67.01±0.34	66.16±1.12
EEGConformer	54.19±2.57	87.24±2.06	73.11±1.95	67.20±2.31	83.89±2.64
EEG2Rep (Default)	53.61±2.07	91.22±1.23	69.77±2.03	68.95±2.89	84.91±3.07
EEG2Rep (Pre-Trained)	59.42 ±1.45	94.13±2.17	<u>74.40</u> ±1.50	<u>75.08</u> ±1.21	88.43 ±3.09
KnowEEG	<u>55.29</u> ±2.58	96.72 ±0.21	85.96 ±0.8	78.28 ±0.56	<u>87.71</u> ±0.23

4.5. KnowEEG Explainability Analysis

Here, we analyse the KnowEEG model trained on the training and validation sets for the Crowdsource dataset and demonstrate the key explainability benefits. The Crowdsource task presents the problem of binary classification on 14-channel EEG data. The two classes are eyes open and eyes closed. For interpretability, we propose analysing the connectivity and statistical features separately.

In hyperparameter selection, Functional Power Connectivity (FPC) was selected as the connectivity measure for the Crowdsource dataset. As defined in Appendix B, the FPC feature set is calculated between each electrode pair over six defined frequency bands (alpha, theta, delta, sigma, beta, gamma) as well as having additional features indicating relative band power values per electrode. The FPC features therefore describe both band power activity and functional connectivity across the brain.

A first step in analysing these feature importances is to plot their distribution. Figure 2 shows an exponential like feature distribution with many feature importances with low values close to zero and fewer and fewer features with higher importances.

We propose as a simple next step to analyse connectivity feature importances per power band. Due to interactions between features, summing feature importances per band does not accurately represent group feature importance [34]. Therefore, instead we compare each channel-channel connectivity measure per band and rank them. For example, electrodes AF3-AF4 will have 6 FPC connectivity values, one for each band. The band with the highest feature importance for each electrode-electrode pair receives a score of 5 down to 6th place which receives a score of 0. The per band ranking feature importance scores are shown in figure 3.

Per figure 3, the Functional Power Connectivity features on the gamma band have the highest importance followed by alpha and then delta, beta, theta and sigma with the lowest importance rank. This suggests that FPC features in gamma and alpha bands are most discriminative versus other bands for eyes closed versus eyes open classification. We can take this analysis further by visualizing FPC features for alpha and gamma for the two classes. We can do this on a surface plot of the 14 electrodes on the head, with the FPC band power features separated from FPC pure connectivity features. We plot FPC band power in figure 4 and connectivity in figure 5.

Per figure 4 the mean eyes open alpha band power is noticeably higher in the eyes closed group vs. eyes open, particularly in the Occipital electrodes

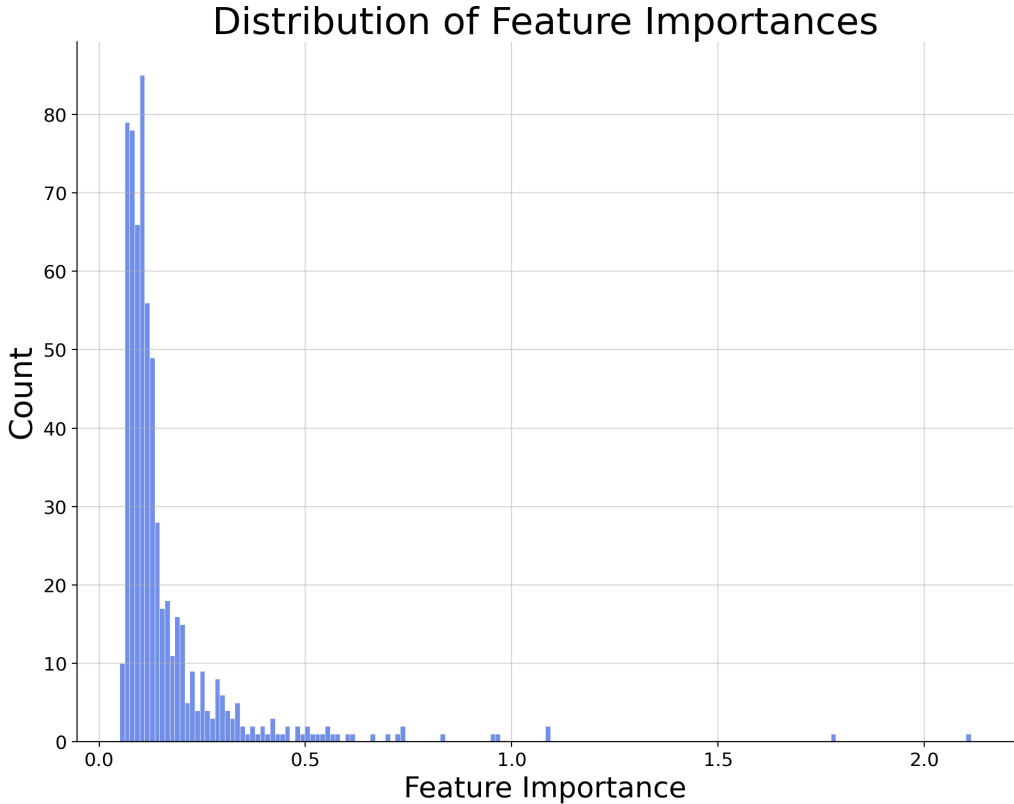


Figure 2: This histogram displays the Gini importance values for the Functional Power Connectivity features (FPC) used by the trained KnowEEG model on the Crowdsource dataset. The x-axis represents the feature importance score with the y-axis showing the count of features at that importance level. The distribution is highly skewed with an exponential-like decay, showing that a large majority of features have an importance score near zero, while a small group of features have higher importance scores.

towards the back of the head. This result is in line with the neuroscience literature that show an increase in alpha power in the eyes closed state [35, 36]. Contrastively the mean gamma band power is significantly higher across the head for the eyes open state vs. eyes closed per figure 4. Again, this is an expected result supported by EEG studies [37]. The eyes being open increases alertness and raises arousal in the brain resulting in stronger activity in the gamma band.

Figure 5 shows that mean FPC alpha connectivity is higher for the eyes closed participants vs. eyes open. This phenomenon is known as alpha de-

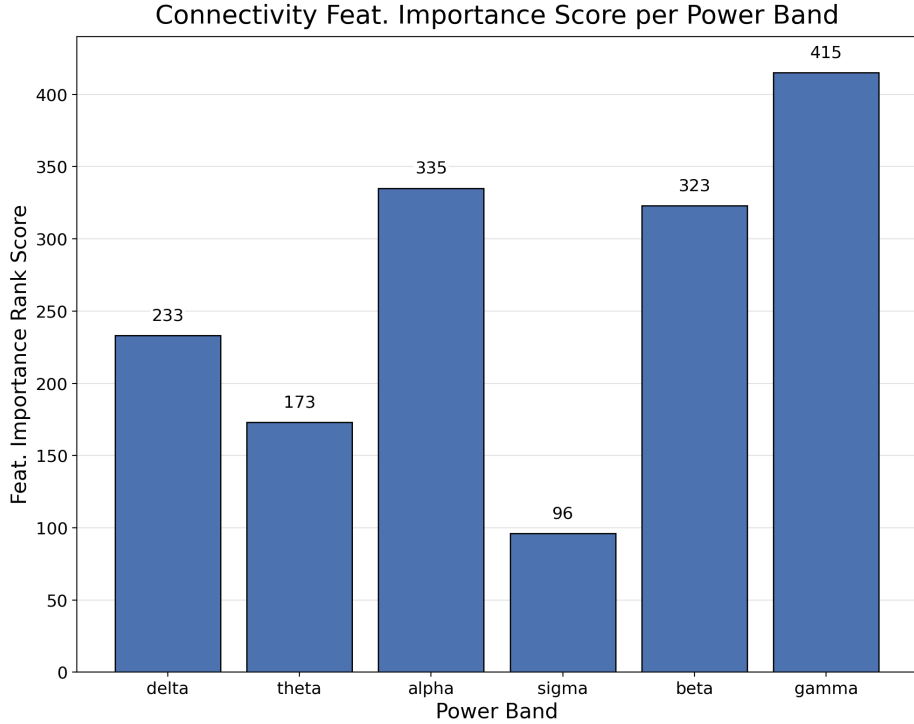


Figure 3: Feature Importance score per power band for Functional Power Connectivity on the Crowdsource dataset. FPC gamma features have the highest feature importance rank score overall followed by alpha, delta, theta and sigma with the lowest score.

synchronization and is consistent with EEG literature that shows "functional connectivity in the alpha band decreases in the eyes open condition compared to eyes closed" [35]. Mean FPC gamma connectivity does not show significant differences between the eyes open and closed groups. This likely reflects the low amplitude and high variability of resting-state gamma activity, making gamma band connectivity a weak discriminator for distinguishing between the eyes open and closed states.

In summary, from our analysis of the Functional Power Connectivity features we have uncovered known neuroscience knowledge. Specifically, we have found increased mean alpha band activity and connectivity in the eyes closed state compared to eyes open as well as increased mean gamma band activity in the eyes open class [35, 38, 37, 36]. This ability of our pipeline to uncover knowledge about the classes is a significant strength. We must note though, that the summary plots showing mean values across the head for both classes

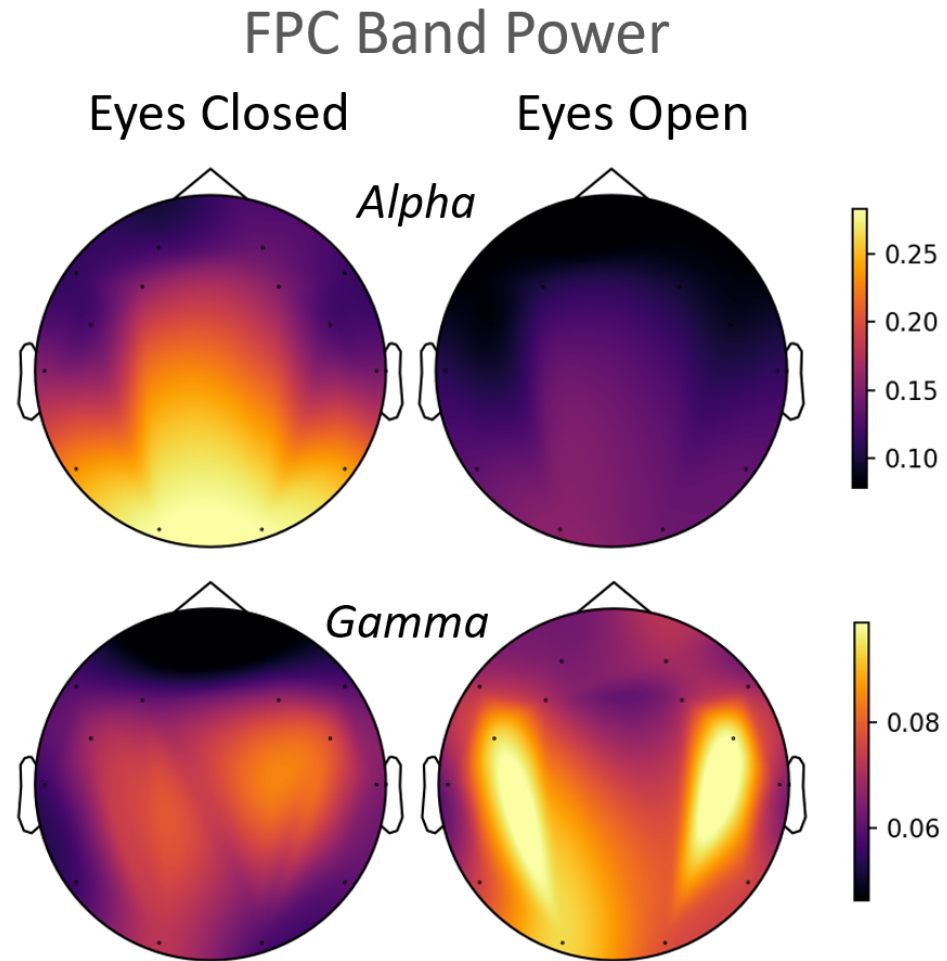


Figure 4: This plot shows mean relative band power in the alpha and gamma bands for eyes closed (left) and eyes open (right) participants. For the Alpha band the eyes closed group have a higher mean power particular in the Occipital Lobes towards the back of the head. For the Gamma band the eyes open group have a higher mean power with peaks in the Left and Right Temporal / Central regions of the brain.

will not always show a clear distinction between classes. However, they are a useful summary view of the features and the detailed KnowEEG feature importance scores will always be available to guide more detailed analysis of the classes.

Furthermore, a granular per channel analysis could also be completed to determine if the connectivity between any channel pairs is particularly

FPC Connectivity

Eyes Closed Eyes Open

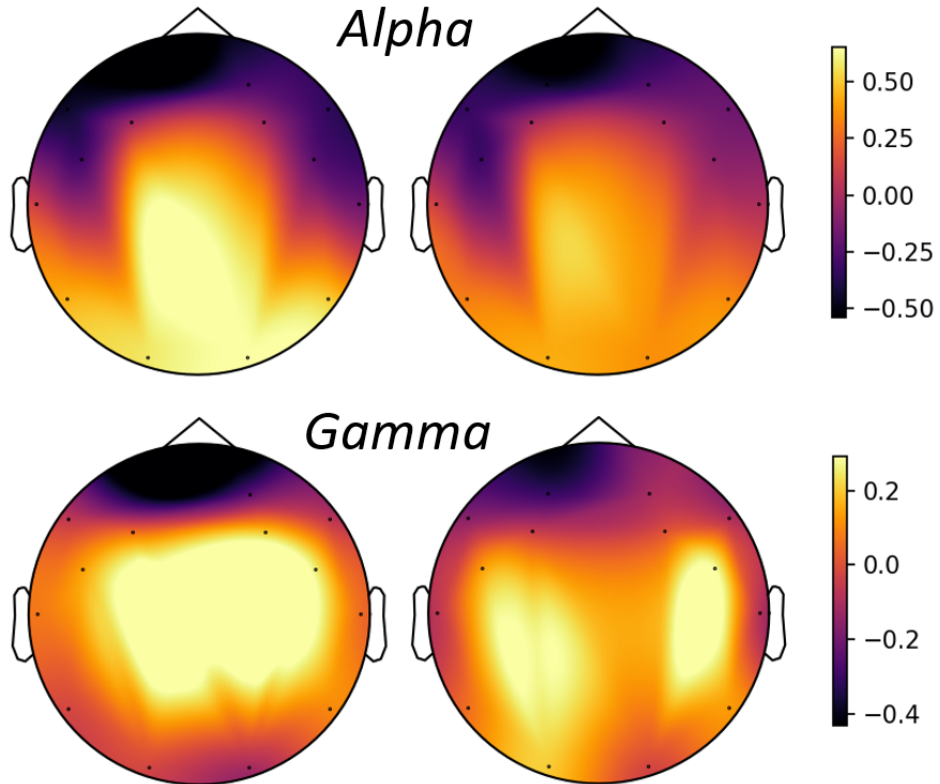


Figure 5: This plot shows the mean Alpha and Gamma band connectivity for the eyes closed (left) and eyes open (right) groups per the FPC features (defined in Appendix B). The eyes closed group have higher Alpha connectivity across the brain particularly in the Occipital regions. For Gamma connectivity the differences between the groups are not visually significant.

discriminative for the classification problem. To keep the analysis focused we move on to the per channel statistical features.

The feature importances for per channel statistics also follow an exponential-like distribution with many features having small importances close to 0 and fewer features having higher importances. As a simple first step we can analyse the top n features by feature importance. We select $n = 10$ features presenting these features in Table 3 below.

Table 3: Statistical features with highest importance ranked 1 to 10. The table displays the feature name, parameters specifying feature calculation, corresponding electrode and corresponding brain region. It is notable that the top 7 features are all from the Occipital brain region.

Rank	Feature	Parameters	Channel	Brain Region
1	Permutation Entropy	Dimension 6 Tau 1	O1	Occipital
2	Permutation Entropy	Dimension 4 Tau 1	O2	Occipital
3	Permutation Entropy	Dimension 5 Tau 1	O2	Occipital
4	Partial Autocorrelation	Lag 2	O1	Occipital
5	Number Peaks	Support 1	O2	Occipital
6	Permutation Entropy	Dimension 5 Tau 1	O1	Occipital
7	Permutation Entropy	Dimension 3 Tau 1	O2	Occipital
8	Mean Absolute Change	N/A	FC6	Right Central
9	Permutation Entropy	Dimension 7 Tau 1	O1	Occipital
10	Quantile Change Mean	Upper 0.8, Lower 0	FC6	Right Central

From Table 3 it is notable that 7 out of the top 7 highest importance features are from the Occipital brain region. This suggests that the Occipital brain region provides features that are most discriminative of the two classes. The two classes are eyes open and eyes closed. We know from existing neuroscience research that the Occipital region of the brain is responsible for visual processing as it "houses the visual cortex responsible for processing and interpreting visual stimuli" [39]. Therefore, again, from our KnowEEG pipeline we have been able to discover knowledge (signals from the Occipital brain region being most discriminative for the two classes) and have verified this versus existing neuroscience literature. This shows that our pipeline can aid discovery of new information where differences between classes are not yet understood.

We extend this feature importance ranking beyond the top 10 features. In Figure 6 we count how many features from each brain region are within the top 5, 10, 20 and 100 features by feature importance. The Occipital brain regions continues to outscore all other regions in the Top 20 and Top 100 features confirming this finding.

Another interesting finding from Table 3 is that the three highest importance features and 6 of the top 10 are permutation entropy from electrodes in

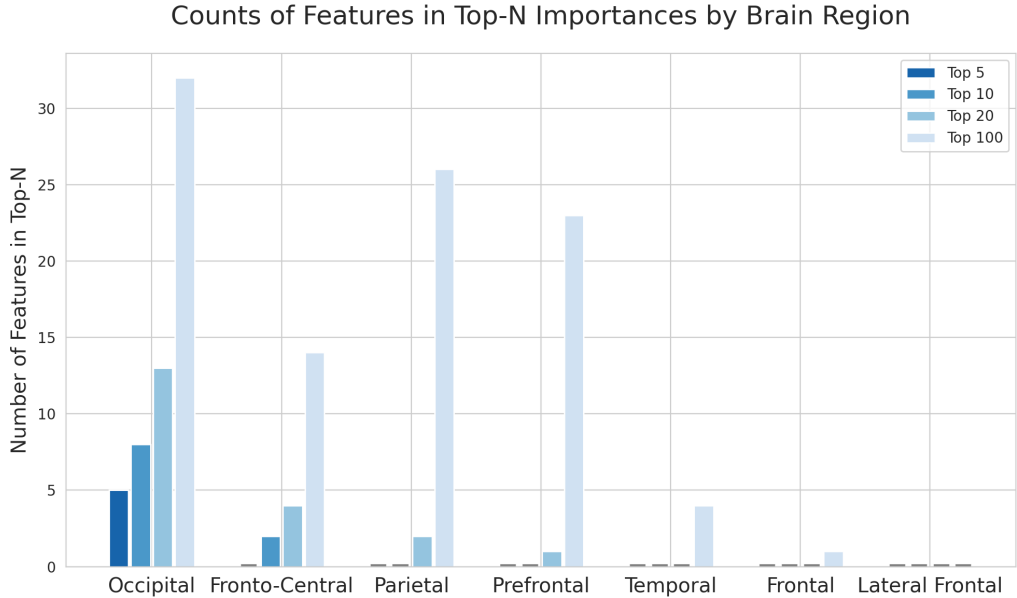


Figure 6: Count of features in top N importances ($N = 5, 10, 20, 100$) by Brain Region. From this bar chart it is clear that the Occipital region has a disproportionately large number of highly discriminative features vs. other regions. The chart shows that 5 out of the top 5 (dark blue) most important features are from the Occipital region as well as 7 of the top 10, 13 of the top 20 and 32 of the top 100.

the Occipital brain region. Permutation entropy is considered as ‘a natural complexity measure for time series’ [40]. The calculation of permutation entropy requires two parameters (Dimension and Tau) which is why this feature can appear multiple times for the same electrode in Table 3.

We plot the Kernel Density Estimates for eyes closed and eyes open for the highest importance ranked feature in Figure 7. It is clear from the figures that the eyes closed group has a much broader distribution compared with the eyes open group. The eyes open group distribution is narrower (standard deviation 0.16 vs 0.47) with a slightly higher peak. When testing the distributions for this feature, we use the two sample Kolmogorov–Smirnov test and find that the two distributions vary significantly ($p\text{-value} < 0.0001$).

Therefore, again our pipeline has enabled us to find out useful information about our classes. In this case that the distributions for permutation entropy on the electrode O1 channel calculated with dimension 6 and tau 1 are significantly different for the eyes closed and eyes open groups.

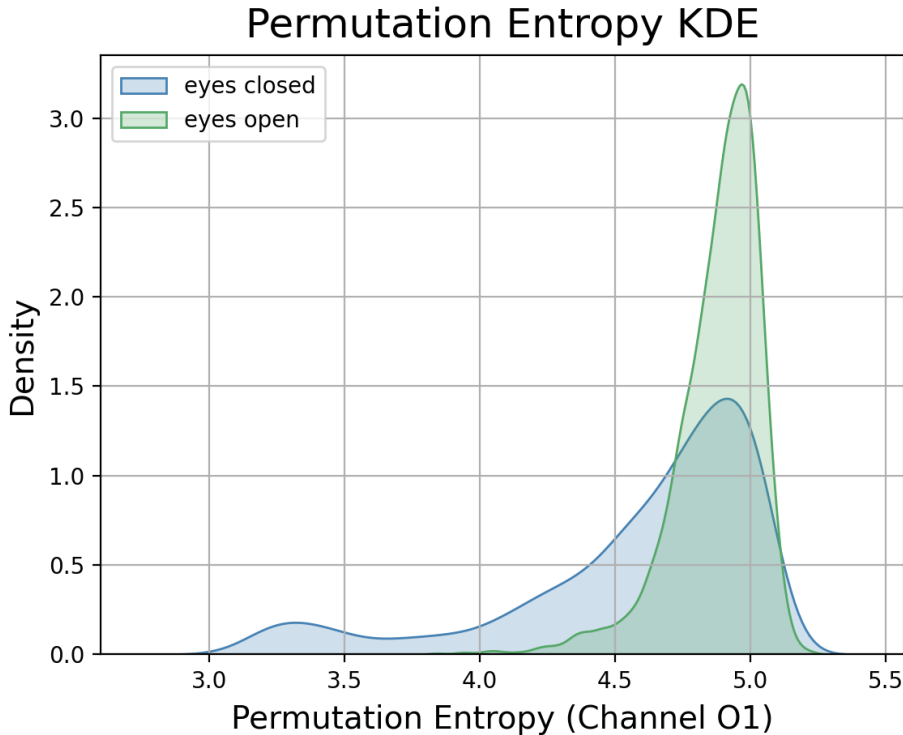


Figure 7: KDE plot of the rank 1 feature from Table 3: Permutation Entropy of the O1 (Occipital Lobe) EEG channel. The distribution for the ‘eyes open’ class (green) is distinctly narrower and has a higher peak density, while the ‘eyes closed’ class (blue) shows a broader distribution with a wider spread of values.

4.6. Benefits and Limitations

Benefits. The main benefit of KnowEEG is the explainability of the model which is in contrast to many state of the art deep learning models. The features themselves have meaning in the generalized time series or EEG domain and the Fusion Forest is a tree-based model that allows users to directly access feature importances. We demonstrate this benefit in 4.5. We show that for the Crowdsourced dataset our explainable pipeline can allow users to discover correct knowledge about the two classes. Notably, we find Occipital Lobe signal statistics as well as gamma band activity, alpha band activity and alpha band connectivity to be discriminative of the eyes open and eyes closed classes. Both findings are confirmed by existing neuroscience literature. Another benefit of our pipeline is high performance across a diverse set of EEG

classification tasks. Versus 7 state-of-the-art baselines on five datasets on 10 performance metrics our pipeline is best on 5/10 metrics, second on 4/10 and outside of the top two models on only 1/10 metrics. Overall, KnowEEG is the best performing model across 5 different EEG datasets. Finally, our pipeline has the significant benefit of not requiring GPU resources for training. The most computationally expensive part of our pipeline is calculation of features that is done on CPU. This means KnowEEG requires fewer specialized resources versus competitor state-of-the-art deep learning models and is therefore more accessible.

Limitations. One limitation is regarding the explainability of KnowEEG. The explanations are only useful if the model itself performs well. If the model performs poorly then the feature importances are likely to provide little insight into the classes. We expect this to be a minor limitation as in our experiments across 5 EEG datasets KnowEEG performed excellently versus competitors. This links closely to the second limitation. The second limitation being that there is no guarantee that KnowEEG performs well across all EEG classification tasks. We have mitigated this risk by extensive experiments across five different EEG datasets with five different classification tasks.

4.7. Future Work

Future work will explore additional EEG datasets to determine if the performance of KnowEEG remains high. This should involve Brain Computer Interface (BCI) EEG datasets such as those discussed in [41]. BCI datasets broadly address the task of enabling a person’s brain signals to communicate with external devices which is distinctly different from the five datasets already explored.

KnowEEG should be deployed on real world data in the healthcare domain to determine if the pipeline can successfully discriminate between classes where the differences between the classes are not already understood. Neurodegenerative diseases such as Alzheimers and Parkinson’s would be a good use case. KnowEEG could potentially uncover previously unknown difference in EEG activity between healthy and diseased individuals furthering advancements in this field.

Further analysis in future work should be done on why KnowEEG outperforms competitors. For example, one could determine what the extent of the shared information between learnt self-supervised representations such

as in EEG2Rep [9] and the features in KnowEEG. This could aid in the development of higher performance models in the future.

5. Conclusion

We present KnowEEG, an explainable high-performance pipeline for EEG classification. We demonstrate through extensive experimentation across five different EEG classification tasks that KnowEEG outperforms state-of-the-art deep learning methods. KnowEEG achieves top or near-top performance across evaluation metrics (accuracy / balanced accuracy and AUROC / W-F1) versus competitor models. KnowEEG has the added benefits of not requiring GPUs for training and is also explainable.

Section 4.5 illustrates the explainability properties of KnowEEG using the Crowdsource dataset. By providing transparent feature importances and interpretable feature representations, KnowEEG allowed us to correctly identify established differences between the two states; reduced alpha synchronisation, elevated alpha-band power, and lower gamma activity during eyes-closed versus eyes-open with statistics from the Occipital-region electrodes most discriminative for classification.

Future work should explore KnowEEG on additional datasets. Furthermore, practitioners should deploy this pipeline on new datasets so that KnowEEG can aid in the discovery of new insights. This could be particularly impactful in domains such as neurodegenerative disease classification where EEG is already being explored as a means of classification.

6. Funding

This work was supported by UK Research and Innovation grant EP/S022937/1: Interactive Artificial Intelligence.

References

- [1] A. J. Casson, M. Abdulaal, M. Dulabh, S. Kohli, S. Krachunov, E. Trimble, Electroencephalogram, Seamless healthcare monitoring: advancements in wearable, attachable, and invisible devices (2018) 45–81.
- [2] A. Sahota, A. Roguski, M. W. Jones, M. Rolinski, A. Whone, R. Santos-Rodriguez, Z. S. Abdallah, Interpretable classification of early stage parkinson’s disease from eeg, in: AI for Health Equity and Fairness:

Leveraging AI to Address Social Determinants of Health, Springer, 2024, pp. 219–231.

- [3] R. Abiri, S. Borhani, E. W. Sellers, Y. Jiang, X. Zhao, A comprehensive review of eeg-based brain–computer interface paradigms, *Journal of neural engineering* 16 (1) (2019) 011001.
- [4] S. Katsigiannis, N. Ramzan, Dreamer: A database for emotion recognition through eeg and ecg signals from wireless low-cost off-the-shelf devices, *IEEE journal of biomedical and health informatics* 22 (1) (2017) 98–107.
- [5] M. Chaturvedi, F. Hatz, U. Gschwandtner, J. G. Bogaarts, A. Meyer, P. Fuhr, V. Roth, Quantitative eeg (qeeg) measures differentiate parkinson’s disease (pd) patients from healthy controls (hc), *Frontiers in aging neuroscience* 9 (2017) 3.
- [6] N. Betrouni, A. Delval, L. Chaton, L. Defebvre, A. Duits, A. Moonen, A. F. Leentjens, K. Dujardin, Electroencephalography-based machine learning for cognitive profiling in parkinson’s disease: Preliminary results, *Movement Disorders* 34 (2) (2019) 210–217.
- [7] S. L. Oh, Y. Hagiwara, U. Raghavendra, R. Yuvaraj, N. Arunkumar, M. Murugappan, U. R. Acharya, A deep learning approach for parkinson’s disease diagnosis from eeg signals, *Neural Computing and Applications* 32 (2020) 10927–10933.
- [8] Y. Song, Q. Zheng, B. Liu, X. Gao, Eeg conformer: Convolutional transformer for eeg decoding and visualization, *IEEE Transactions on Neural Systems and Rehabilitation Engineering* 31 (2023) 710–719. doi:10.1109/TNSRE.2022.3230250.
- [9] N. Mohammadi Foumani, G. Mackellar, S. Ghane, S. Irtza, N. Nguyen, M. Salehi, Eeg2rep: Enhancing self-supervised eeg representation through informative masked inputs, in: *Proceedings of the 30th ACM SIGKDD Conference on Knowledge Discovery and Data Mining, KDD ’24*, Association for Computing Machinery, New York, NY, USA, 2024, p. 5544–5555. doi:10.1145/3637528.3671600.
URL <https://doi.org/10.1145/3637528.3671600>

- [10] C. Ieracitano, N. Mammone, A. Hussain, F. C. Morabito, A novel explainable machine learning approach for eeg-based brain-computer interface systems, *Neural Computing and Applications* 34 (14) (2022) 11347–11360.
- [11] C. H. Lubba, S. S. Sethi, P. Knaute, S. R. Schultz, B. D. Fulcher, N. S. Jones, *catch22: Canonical time-series characteristics: Selected through highly comparative time-series analysis*, *Data Mining and Knowledge Discovery* 33 (6) (2019) 1821–1852.
- [12] D. M. Groppe, S. Bickel, C. J. Keller, S. K. Jain, S. T. Hwang, C. Harden, A. D. Mehta, Dominant frequencies of resting human brain activity as measured by the electrocorticogram, *Neuroimage* 79 (2013) 223–233.
- [13] Y. Kuang, Z. Wu, R. Xia, X. Li, J. Liu, Y. Dai, D. Wang, S. Chen, Phase lag index of resting-state eeg for identification of mild cognitive impairment patients with type 2 diabetes, *Brain Sciences* 12 (10) (2022) 1399.
- [14] G. Chiarion, L. Sparacino, Y. Antonacci, L. Faes, L. Mesin, Connectivity analysis in eeg data: A tutorial review of the state of the art and emerging trends, *Bioengineering* 10 (3) (2023) 372.
- [15] S. Waninger, C. Berka, M. Stevanovic Karic, S. Korszen, P. D. Mozley, C. Henchcliffe, Y. Kang, J. Hesterman, T. Mangoubi, A. Verma, Neurophysiological biomarkers of parkinson’s disease, *Journal of Parkinson’s disease* 10 (2) (2020) 471–480.
- [16] C. Li, Y. Qi, X. Ding, J. Zhao, T. Sang, M. Lee, A deep learning method approach for sleep stage classification with eeg spectrogram, *International Journal of Environmental Research and Public Health* 19 (10) (2022) 6322.
- [17] B. Mandhoudj, M. A. Cherni, M. Sayadi, An automated classification of eeg signals based on spectrogram and cnn for epilepsy diagnosis, *Analog integrated circuits and signal processing* 108 (1) (2021) 101–110.
- [18] Y. Song, Q. Zheng, B. Liu, X. Gao, Eeg conformer: Convolutional transformer for eeg decoding and visualization, *IEEE Transactions on Neural Systems and Rehabilitation Engineering* 31 (2022) 710–719.

- [19] R. T. Schirrmeister, J. T. Springenberg, L. D. J. Fiederer, M. Glasstetter, K. Eggensperger, M. Tangermann, F. Hutter, W. Burgard, T. Ball, Deep learning with convolutional neural networks for eeg decoding and visualization, *Human brain mapping* 38 (11) (2017) 5391–5420.
- [20] W. Weng, Y. Gu, S. Guo, Y. Ma, Z. Yang, Y. Liu, Y. Chen, Self-supervised learning for electroencephalogram: A systematic survey, *arXiv preprint arXiv:2401.05446* (2024).
- [21] D. Kostas, S. Aroca-Ouellette, F. Rudzicz, Bendl: Using transformers and a contrastive self-supervised learning task to learn from massive amounts of eeg data, *Frontiers in Human Neuroscience* 15 (2021) 653659.
- [22] C. Yang, M. Westover, J. Sun, Biot: Biosignal transformer for cross-data learning in the wild, *Advances in Neural Information Processing Systems* 36 (2024).
- [23] M. Christ, N. Braun, J. Neuffer, A. W. Kempa-Liehr, Time series feature extraction on basis of scalable hypothesis tests (tsfresh—a python package), *Neurocomputing* 307 (2018) 72–77.
- [24] Y. Benjamini, D. Yekutieli, The control of the false discovery rate in multiple testing under dependency, *Annals of statistics* (2001) 1165–1188.
- [25] A. Gramfort, M. Luessi, E. Larson, D. A. Engemann, D. Strohmeier, C. Brodbeck, R. Goj, M. Jas, T. Brooks, L. Parkkonen, et al., Meg and eeg data analysis with mne-python, *Frontiers in Neuroinformatics* 7 (2013) 267.
- [26] D. R. Edla, K. Mangalorekar, G. Dhavalikar, S. Dodia, Classification of eeg data for human mental state analysis using random forest classifier, *Procedia computer science* 132 (2018) 1523–1532.
- [27] L. Fraiwan, K. Lweesy, N. Khasawneh, H. Wenz, H. Dickhaus, Automated sleep stage identification system based on time–frequency analysis of a single eeg channel and random forest classifier, *Computer methods and programs in biomedicine* 108 (1) (2012) 10–19.

- [28] W. L. Lim, O. Sourina, L. P. Wang, Stew: Simultaneous task eeg workload data set, *IEEE Transactions on Neural Systems and Rehabilitation Engineering* 26 (11) (2018) 2106–2114.
- [29] N. S. Williams, W. King, G. Mackellar, R. Randeniya, A. McCormick, N. A. Badcock, Crowdsourced eeg experiments: A proof of concept for remote eeg acquisition using emotivpro builder and emotivlabs, *Heliyon* 9 (8) (2023).
- [30] S. López, G. Suarez, D. Jungreis, I. Obeid, J. Picone, Automated identification of abnormal adult eegs, in: *2015 IEEE Signal Processing in Medicine and Biology Symposium (SPMB)*, 2015, pp. 1–5. doi:10.1109/SPMB.2015.7405423.
- [31] A. Harati, M. Golmohammadi, S. Lopez, I. Obeid, J. Picone, Improved eeg event classification using differential energy, in: *2015 IEEE Signal Processing in Medicine and Biology Symposium (SPMB)*, 2015, pp. 1–4. doi:10.1109/SPMB.2015.7405421.
- [32] H.-Y. S. Chien, H. Goh, C. M. Sandino, J. Y. Cheng, Maeeg: Masked auto-encoder for eeg representation learning, *arXiv preprint arXiv:2211.02625* (2022).
- [33] M. Grandini, E. Bagli, G. Visani, Metrics for multi-class classification: an overview, *arXiv preprint arXiv:2008.05756* (2020).
- [34] I. Covert, S. M. Lundberg, S.-I. Lee, Understanding global feature contributions with additive importance measures, in: H. Larochelle, M. Ranzato, R. Hadsell, M. Balcan, H. Lin (Eds.), *Advances in Neural Information Processing Systems*, Vol. 33, Curran Associates, Inc., 2020, pp. 17212–17223.
- [35] J. Gómez-Ramírez, S. Freedman, D. Mateos, J. L. Pérez-Velázquez, T. Valiante, Eyes closed or eyes open? exploring the alpha desynchronization hypothesis in resting state functional connectivity networks with intracranial eeg, *bioRxiv* (2017). arXiv:<https://www.biorxiv.org/content/early/2017/03/18/118174.full.pdf>, doi:10.1101/118174.
URL <https://www.biorxiv.org/content/early/2017/03/18/118174>

- [36] R. J. Barry, A. R. Clarke, S. J. Johnstone, C. A. Magee, J. A. Rushby, Eeg differences between eyes-closed and eyes-open resting conditions, *Clinical neurophysiology* 118 (12) (2007) 2765–2773.
- [37] A. S. Geller, J. F. Burke, M. R. Sperling, A. D. Sharan, B. Litt, G. H. Baltuch, T. H. Lucas II, M. J. Kahana, Eye closure causes widespread low-frequency power increase and focal gamma attenuation in the human electrocorticogram, *Clinical Neurophysiology* 125 (9) (2014) 1764–1773.
- [38] D. Kan, P. Croarkin, C. Phang, P. Lee, Eeg differences between eyes-closed and eyes-open conditions at the resting stage for euthymic participants, *Neurophysiology* 49 (6) (2017) 432–440.
- [39] A. Abd-Elsayed, *Basic Anesthesia Review*, Oxford University Press, 2024. doi:10.1093/med/9780197584569.001.0001.
URL <https://doi.org/10.1093/med/9780197584569.001.0001>
- [40] C. Bandt, B. Pompe, Permutation entropy: a natural complexity measure for time series, *Physical review letters* 88 (17) (2002) 174102.
- [41] H. Cho, M. Ahn, S. Ahn, M. Kwon, S. C. Jun, Eeg datasets for motor imagery brain–computer interface, *GigaScience* 6 (7) (2017) gix034. doi:10.1093/gigascience/gix034.
- [42] F. Pedregosa, G. Varoquaux, A. Gramfort, V. Michel, B. Thirion, O. Grisel, M. Blondel, P. Prettenhofer, R. Weiss, V. Dubourg, et al., Scikit-learn: Machine learning in python, *Journal of machine learning research* 12 (Oct) (2011) 2825–2830.

Appendix A. KnowEEG Set Up

The TSFresh [23] python package with version 0.20.3 was used to calculate the per electrode statistics with ‘Efficient’ setting for feature calculation. The MNE python package [25] version 1.7.1 was used to calculate the connectivity metrics, further details on connectivity metrics are provided in appendix Appendix C. The python package Scikit-learn [42] with version 1.6.1 was used to generate the trees of the Fusion Forest. Decision trees with default hyperparameter settings were used for the Fusion Forest (criterion =‘gini’, max depth=None, min samples split =2, min samples leaf = 1, max features = None).

Appendix B. Functional Power Connectivity

In addition to correlation and conventional phase / coherence based connectivity measures we introduce an amplitude-based functional connectivity set of features which we term Functional Power Connectivity (FPC). For each electrode and frequency band (delta, theta, alpha, sigma, beta, gamma) we compute relative bandpower. We then define FPC features as the pairwise log-ratios of relative bandpower between electrodes.

Therefore for each band between each electrode pair i,j we compute :

$$FPC_{i,j} = \log P_i^{\text{rel}} - \log P_j^{\text{rel}} = \log \left(\frac{P_i^{\text{rel}}}{P_j^{\text{rel}}} \right) \quad (B.1)$$

This means for a set of 14 electrodes there are in total 630 total FPC features comprising 6×14 band power features plus 91×6 bands of electrode-electrode features. These features capture regional band power as well as spatial differences in oscillatory power across regions which can be interpreted as power-based functional connectivity markers.

Appendix C. Connectivity Metrics Overview

Connectivity metrics for KnowEEG were selected using literature and are not exhaustive [25] [13] . The selected metric is a hyperparameter of the pipeline. Therefore users can add metrics to their pipeline that they expect to be informative.

Correlation is calculated in the time domain using the entire EEG signal. This results in a channel-channel matrix of features. As we calculate Pearson and Spearman correlation this leads to two channel-channel matrices of features. All other connectivity measures are calculated across the six power bands (delta, theta, alpha, sigma, beta, gamma). Therefore they result in six channel-channel matrices of features. For example for Phase Lag Index (PLI) this would lead to PLI on the delta band for each channel-channel pair, PLI on the theta band for each channel-channel pair etc...

Some metrics such as Phase Lag Index require segmentation of the EEG signal in order to determine how properties of the signal vary over time. Selected metrics for the pipeline are therefore split into those requiring and not requiring segmentation.

The MNE package was used for all connectivity metric calculations (except for correlation) and can therefore be referred to for exact definitions [25]. We use the same names below as in the MNE package.

Selected Metrics (no segmentation required) are:

- Correlation (Pearson and Spearman correlation, considered together as a single metric)
- Functional Power Connectivity

Selected Metrics (with signal segmentation) are:

- Coherence
- Imaginary Coherence
- Pairwise Phase Consistency
- Phase Lag Value
- Phase Lag Index
- Directed Phase Lag Index
- Weighted Phase Lag Index

In table C.4 below we show for the metrics with signal segmentation how the signal was segmented for each dataset. There is a trade-off between the length of each segment and number of segments in calculation of each metrics. More segments will lead to a more accurate calculation of the metric. However, a long enough segment is required in order to provide enough signal, particularly for lower frequency components of the signal.

For DREAMER, STEW, and Crowdsourced due to the short nature of the signals, segmented metrics in the lower frequency bands are unlikely to contain useful information. However, for completeness we calculate them and allow KnowEEG to select from calculated metrics.

Appendix D. Datasets

Datasets and preprocessing follow the same protocol as in [9].

Dataset	Signal Duration	Freq	Segment Duration	Num Segments
DREAMER	2s	128Hz	0.25	8
STEW	2s	128Hz	0.25	8
Crowdsourced	2s	128Hz	0.25	8
TUEV	5s	256Hz	0.50	10
TUAB	10s	256Hz	0.625	16

Table C.4: Overview of segmentation for signals for each dataset. Required in order to calculate specific connectivity metrics (Coherence, Imaginary Coherence, Pairwise Phase Consistency, Phase Lag Value, Phase Lag Index, Directed Phase Lag Index, Weighted Phase Lag Index).

Appendix D.1. Emotiv datasets

All Emotiv datasets were bandpass filtered and windowed into segments of length 256. This data is recorded at a sampling rate of 128Hz. Therefore, each segment is of 2 seconds in length.

DREAMER

The DREAMER [4] dataset is a multimodal database containing both electroencephalogram (EEG) and electrocardiogram (ECG) signals. These signals are recorded during affect elicitation with audi-visual stimuli [4]. Data is recorded from 23 participants along with self-assessment of affective state after each stimuli. Self assessment is in terms of valence, arousal and dominance. For classification we use the arousal labels as per [9]. We utilize the toolkit Torcheeg for preprocessing which consists of low-pass and high-filters. We do not use the ECG data and use only the EEG data. The DREAMER dataset can be accessed here¹.

Crowdsource

The Crowdsourced [35] dataset was recorded with participants at rest in the eyes closed or eyes open state. Each recording is 2 minutes in total. There are 60 total participants with only 13 recording data for both states.

¹<https://zenodo.org/records/546113>

Data is recorded using 14-channel EPOC devices and is initially recorded at 2048Hz and then downsampled to 128Hz. This data can be accessed via the Open Science Framework ²

Simultaneous Task EEG Workload (STEW)

The STEW dataset [28] is an open access EEG dataset for multitasking and mental workload analysis. There are 48 total subjects and data is recorded using a 14-channel Emotiv EPOC headset. Data is recorded for subjects at baseline (rest) and under workload in the SIMKAP mutitasking setting. EEG recordings are of length 2.5 minutes and recorded at 128Hz. Participants recorded their perceived mental workload on a scale of 1 to 9. STEW also has binary labels recording workload of above 4 as high and below 4 as low. These binary labels are used for our classification task. STEW is accessible via the IEEE DataPort ³.

Appendix D.2. Temple University Hospital (TUH) Datasets

The TUH EEG Events dataset (TUEV) [31] and the TUH Abnormal EEG corpus (TUAB) [30] are accessible on request from the Neural Engineering Data Consortium (NEDC) here ⁴. The TUH datasets were processed in accordance with standard 16 EEG montages [9] and the 10-20 international system with: "FP1-F7", "F7-T7", "T7-P7", "P7-O1", "FP2-F8", "F8-T8", "T8-P8", "P8-O2", "FP1-F3", "F3-C3", "C3-P3", "P3-O1", "FP2-F4", "F4-C4", "C4-P4", and "P4-O2".

TUH Events Corpus (TUEV)

The TUH EEG Events Corpus (TUEV) [31] [9] contains EEG data with samples segmented into six categories. The categories are spike and sharp wave, eye movement, artifact, background generalized periodic epileptiform discharges and periodic lateralized epileptiform discharges [31].

TUH Abnormal EEG Corpus (TUAB)

The TUH Abnormal EEG Corpus (TUAB) [30] [9] is a large-scale corpus of EEGs recordings designed to support research on automated EEG interpretation. This corpus is drawn from a diverse group of subjects with EEG labeled as either normal or abnormal [30].

²<https://osf.io/9bvgħ/>

³<https://ieee-dataport.org/open-access/stew-simultaneous-task-eeg-workloaddataset>

⁴https://isip.piconepress.com/projects/nedc/html/tuh_eeg/